NAVORD REPORT 2954

DRAG AND EVAPORATION OF DRY ICE MODELS IN SUPERSONIC AIR FLOW

21 SEPTEMBER 1953

U. S. NAVAL ORDNANCE LABORATORY
WHITE OAK, MARYLAND

UNCLASSIFIED
NAVORD Report 2854

Aeroballistic Research Report 189

DRAG AND EVAPORATION OF DRY ICE MODELS IN SUPERSONIC AIR FLOW

By:

K. B. Gruenewald

ABSTRACT: Investigations on drag and evaporation of dry ice models were conducted in the NOL 40 x 40 cm Aerobalistics Tunnel No. 2. The drag coefficient was determined for dry ice spheres at Mach numbers 2.9 and 4.3, and the rate of evaporation of dry ice was investigated on cubes and spheres at Mach numbers 1.9, 2.9 and 4.3. The drag coefficient was found to be essentially the same as that of usual nonevaporative wind-tunnel models of the same geometric shape. Most of the evaporation during a blow occurred at the front portion of the model. In this wind tunnel the mass loss caused by evaporation becomes smaller as the Mach number is increased due to the lower density of the air in the test section at higher Mach numbers. Furthermore, the mass loss per unit cross-sectional area of the model decreases with increasing model size.

U. S. NAVAL ORDNANCE LABORATORY
WHITE OAK, MARYLAND

NAVORD Report 2954 21 September 1953

This report presents results of experiments on evaporating models. The investigation was suggested by Prof. F. L. Whipple, Harvard University, Cambridge, Massachusetts, in connection with his studies on meteors. The results of this investigation have been evaluated with respect to their application to astrophysical phenomena by R. N. Thomas and F. L. Whipple and are partially published in references (a) and (b). Since experimental results on evaporating models may also be of interest to problems of missile cooling, the investigation on dry ice models is presented in all details in this report.

This investigation was made under NOL task number Re9a-108. The measurements were carried out at the Naval Ordnance Laboratory in the 40 x 40 cm Aeroballistics Tunnel No. 2 in 1950.

The author wishes to express his gratitude to Mr. J. M. Kendall and Mr. J. L. Ettle who worked out the technique of manufacturing the dry ice models and who prepared all the models used during this investigation. The author acknowledges the help of Mr. M. Peucker in preparing the drag balance.

EDWARD L. FOODYARD
Captain, USN
Commander

R. N. KURZWEG, Chief
Aeroballistic Research Department
By direction

CONTENTS

TABLES AND ILLUSTRATIONS

DRAG AND EVAPORATION OF DRY ICE MODELS IN SUPERSONIC AIR FLOW

I. INTRODUCTION

1. A theory for determining air densities at high altitudes from meteoric data has been developed by F. L. Whipple (reference c). The application of this theory requires the knowledge of the numerical values of two quantities, namely aerodynamic drag and mass loss of meteors which have to be estimated. In order to substantiate the quantitative aspect of this theory, Professor Whipple (reference d) suggested the experimental investigation of evaporation rate and drag of vaporizing models in a supersonic wind tunnel. An accuracy of the test results within 50 per cent of the actual values was considered sufficient to satisfy the theory.

2. The temperature of the atmosphere at 50 km altitude amounts to about 300°K. For a meteor traveling at a speed of 50 km/sec at this altitude (reference e), the stagnation temperature of the air is approximately 10^{5}°K (reference f). The temperature of the meteor was assumed to be 2000°K, and the meteor was considered to vaporize from the solid state (sublimation) (reference d). In order to simulate these conditions at low temperatures, dry ice (solid CO_2) was chosen as the model material for the wind-tunnel measurements. Dry ice has a sublimation point of 194.7°K at 1 atm (reference g), which is intermediate between the wind-tunnel stagnation temperature of about 300°K and the static temperature of the air flow (177°K for Mach number 1.56 to about 50°K for Mach number 5.0).

II. TEST ARRANGEMENT

3. The investigation was performed in the NOL 40 x 40 cm Aerobalistics Tunnel No. 2 (reference h). For this tunnel the air is taken from the atmosphere, passed through a dryer which dries to a dewpoint of approximately -30°C, expanded in a Laval nozzle, and discharged through a supersonic diffuser into a vacuum vessel of 2000 m^{3} volume. The tunnel is of the

intermittent type with 40 to 60 seconds blowing time and has a nozzle exit cross section of 40 x 40 cm. The Mach numbers and models investigated are shown in Table I.

TABLE I

INVESTIGATED DRY ICE MODELS

Mach Number	Sphere Diameter in mm			Cube Side Length in mm		
1.86	30	50[x]	--	30[x]	50[x]	--
2.87	30	50	70[x]	30[x]	50[x]	70[x]
4.25	--	50	--	--	--	--

x) Evaporation rate measurements only

4. High Mach numbers with low air densities would best simulate the conditions encountered by missiles in the upper atmosphere. However, at Mach number 4.25, the highest Mach number used, the duration of a tunnel blow was already too short to produce a mass loss sufficiently great to cause a visible change in the model shape. Drag measurements have been obtained in two cases only, since in the course of the investigation the balance for the drag measurements become inoperative. The mass loss was determined in all cases.

5. The dry ice model was mounted on a precooled holder of small heat conductivity (bakelite) in order to reduce evaporation of dry ice by heat conduction through the holder. The holder covered the front portion of an axial force balance having 5 kg load capacity (Figure 1). The spring deflection during the blow caused by the air forces effects the resistance of the strain gages attached to the springs. The current due to the change of the resistance was measured by a GE potentiometer recorder. The balance was calibrated with model-holder and a ring of dry ice around the holder screw provided to hold the model. In this manner errors caused by the low temperature of the dry ice model were eliminated as far as possible.

6. The mass loss due to the vaporization during the blow was determined by weighing the models before and after the blow. This loss was corrected by the mass loss experienced during an equal handling period without blast.

III. TEST PROCEDURE

A. Manufacturing of the models

7. The dry ice was sawed into cubes and in each cube a hole with threads was cut using a tap precooled in a mixture of dry ice and alcohol. Then the cube was screwed on a precooled sting of bakelite mounted on a lathe and was cut to a sphere with a knife.

B. Test

8. The model was weighed quickly lying on filter paper in order to reduce mass loss due to heat conduction to the scales. At the moment the weight was determined a stop clock was turned on. After the diameter of the model had been measured with a caliper, the model was screwed on the precooled bakelite sting covering the front portion of the balance. (This sting was precooled by an attached dry ice piece.) Then the balance was adjusted and the blow started. Another stop clock measured the blow time. The drag was recorded during the blow with the GE recorder. After the blow the model was taken out of the tunnel and weighed again. The stop clock was turned off when this second weighing was finished. Finally the diameter of the model was measured again. The time between the end of the blow and the end of the second weighing was determined with a watch. Supply air pressure and temperature were measured for the determination of the drag coefficient.

C. Mass loss without blow

9. The procedure for determining the mass loss without blow was the same as just described but without blow and drag measurements. This mass loss was determined for cubes and spheres with different side lengths or diameters and also for different evaporation times.

IV. DATA REDUCTION

10. The drag coefficient of the model was determined at the start and the end of the blow only and the evaporated mass was determined for the time duration of one blow. The following steps were taken for this procedure:

A. Diameter at start and end of the test

11. The model diameter at the start and the end of the test (first and last weighing of the model) was measured by a caliper. These measurements are inaccurate in so far as the caliper melts dry ice during the time it touches the model and therefore indicates a diameter smaller than the actual diameter. The inaccuracy is larger for spheres than for cubes because the caliper touches the sphere in two points, which melt quickly, but touches the cube along two sides which melt more slowly. This was confirmed by comparison of the measured diameters of the spheres with the diameters calculated from the weight of the models at the test start under the assumption that the models were true spheres and cubes, and taking into account the weight of the sting hole in the models (The specific weight of the dry ice used was determined to be 1.52 g/cm^3.) The calculated side lengths of the cubes agreed with the measured ones within less than 1 per cent; the calculated values of the sphere diameters were about 1 per cent to 2 per cent larger than the measured values. Considering the inaccuracy of the measurements, the calculated values of the diameters were taken at the test start. Since the shape of the models changed unsymmetrically during the blow, only the measured values of the diameter at the end of the test could be used for the data evaluation. However, 0.3 mm corresponding to about 1 per cent of the diameter of the smallest sphere have been added as a correction to the measured values of the sphere diameter according to the above mentioned experience.

B. Diameter at start and end of the blow

12. These diameters were obtained from the diameters at start and end of the test, deducting and adding the experimentally determined diameter decrease for the time while not blowing respectively.

13. This time consists of two parts; the time between the first weighing of the model and the blow start and the time between blow end and second weighing. These time intervals were determined from the blow time, the time between first and second weighing and the time between blow end and second weighing all of which were known.

14. Furthermore, the mass loss of spheres and cubes for times without blow was known. The diameter decrease of the models without blow was determined and is shown in Figure 2. It was obtained from the measured and calculated diameters of the model at the start and the end of the test without blow. Figure 2 shows that the scatter of the calculated values is less than that of the measured values, as explained above. The diameter decrease as a function of the diameter at test start for a constant time interval is shown in Figure 2a. One curve for all models was used since the diameter decrease was found to be independent of the model size within the measuring accuracy. The average scatter of the calculated values is about ±7 per cent.

C. Drag coefficient

15. Since the diameters of the model at the start and the end of the blow are determined, the corresponding cross-section areas A are known. The density ρ and the velocity v of the undisturbed flow were determined from the pressure and temperature of the supply air and the Mach number. The drag coefficient C_D was calculated using the equation:

$$C_D = \frac{F}{\frac{\rho \cdot v^2}{2} A}$$

where F is the drag force.

D. Mass loss while not blowing

16. The mass loss per unit time and unit surface area without blow was found to be the same for cubes and spheres; namely, 0.000283 g/sec. cm^2 ± 6 per cent. However, the mass loss without blow referred to the cross-sectional area is different for cubes and spheres (see Table 3). To facilitate data reduction, the mass loss was referred to the cross-sectional area of the

models since the area perpendicular to the air stream did not change much as compared with that of the model surface during the blow (Figure 3 and Table II). Furthermore, it was difficult to determine the model surface area after the blow.

17. The mass loss for the time between test start and blow start was obtained by multiplying the mass loss without blow (in g/sec. cm^2 area) with the time without blow and with the average cross-sectional area which the model had during this time. The same was done for the time between blow end and test end. Both mass losses added together gave the total mass loss while not blowing. The procedure of determining the mass loss after the blow is somewhat inaccurate because the model shape after the blow is not a sphere or a cube respectively. This procedure was chosen, however, because the average surface area of the model after the blow was very difficult to determine and because the time between blow end and test end was in no case more than 31 per cent of the total time without blow.

a. Mass loss during blow

18. This loss was obtained by deducting the loss while not blowing from the total loss between the two weighings. The mass loss was referred to one second blow time and to one cm^2 of the average cross-sectional area of the model perpendicular to the air stream during blow time.

V. ACCURACY OF THE MEASUREMENTS

19. The calibration of the balance showed that it was influenced by sideforces such as lift and yaw. The measurement obtained from a sideforce was about 20 per cent of the value resulting from a force at the same magnitude acting axially. In spite of this inaccuracy, this balance was used because no other balance was available at that time. Furthermore, since the model shapes at least at the start of the blow were symmetrical with respect to the air stream, any sideforce influence could be considered negligible. The holder influence on the drag measurements could not be eliminated completely but this influence is considered to be small and may be neglected for these models. The approximate accuracies for the mass losses during the blow were calculated with the following assumed errors in determining the test items:

Weight ± 0.1 g

Time between weighings ± 1 sec.

Time without blast between test start and blow start ± 5 sec.

Time without blast between blow end and test end ± 5 sec.

Blow time ± 0.2 sec.

Diameter decrease without blast (as found experimentally) ± 7 per cent

Mass loss without blast per second and cm^2 cross-sectional area (as found experimentally) ± 6 per cent

Diameter at test start and end ± 0.3 mm for spheres

Edge length at test start and end ± 0.1 mm for cubes

The error in the determination of the average cross-sectional area of the models during the blow was calculated to be less than 1 per cent for a cube of 70 mm side length and up to 2.5 per cent for a sphere 30 mm diameter. The mass loss per second and cm^2 of this area was found to be accurate to ± 5 per cent at Mach number 1.86 and up to ± 17 per cent at Mach number 4.25. The measured values of the mass loss for all models and all Mach numbers scatter within ± 11 per cent around the curves drawn in Figure 4. At Mach number 1.86 there exists a distinct difference between cubes (scatter ± 5 per cent) and spheres (scatter ± 16 per cent). The high value of scattering of the spheres may be attributed to loss of pieces broken off from the spheres during the blow. (See values with question marks in Figure 4).

VI. RESULTS

20. The vaporization of dry ice at Mach number 4.25 was so small that no change in model shape could be observed. At the lower Mach numbers 2.87 and 1.86 the evaporation was clearly visible. During evaporation,

the front part of the models assumed a conical shape with a round tip and nicks in case of the spheres and formed sloping areas with nicks in case of the cubes. The rear part of each model remained unchanged. The somewhat non-uniform evaporation at the front part may be caused by inhomogeneities of the polycrystalline structure of the dry ice, due to the mechanical compacting of the snow flakes in making solid dry ice. The shapes of models with 5 cm diameter after the blow are shown in Figure 3 (one cylindrical model, 5 cm long and 3 cm in diameter, was also investigated and is shown in Figure 3). Models 3 cm in diameter showed more erosion of shapes (half spherical shape in the case of spheres), models with 7 cm diameter were less eroded as the models shown in Figure 3.

21. The drag coefficient of dry ice spheres was found to be approximately 1 at Mach numbers 4.25 and 2.87, measured 3 to 4 sec. after the blow started. The coefficient increased 5 per cent at Mach number 4.25 and 16 per cent at Mach number 2.87 during the blow with a duration of about 35 seconds (Table 3). The drag coefficient shortly after blow start is in fair agreement with the drag coefficient of spheres measured in supersonic wind tunnels. The increase of the drag coefficient during the blow can be attributed to the variation of the shape of the model and seems to be unaffected by the evaporation of dry ice surrounding the model. Thus the drag coefficient seems to be the same as found for non-evaporative wind-tunnel models of the same shape. Because the shape changes during the blow from spheres to hemispheres (especially at low Mach numbers), the drag coefficient can be expected to be between 1 and 1.5.

22. The mass loss during the evaporation as a function of the average cross-sectional area of the model during the blow is shown in Figure 4. The values for the spheres and those of the cubes have been found to be approximately equal at each Mach number. Some previous unpublished data by J. M. Kendall and P. P. Wegener of NOL taken at a Mach number of 1.7 in a continuous 2.5 x 2.5 cm wind tunnel are included in Figure 4. The graph shows that the mass loss due to the evaporation of dry ice increases with decreasing Mach number and with decreasing area.

23. The evaporation of dry ice in supersonic air flow may be explained as follows: The evaporation

of dry ice is due to the transfer of heat from the air to the model and to the transfer of evaporated material from the model to the air. The high rate of energy exchange with the oncoming air at the front part of the model causes a great evaporation of dry ice. The evaporating process is supported by the quick replacement of evaporating dry ice molecules by air molecules. The number of air molecules per unit time is a function of air density and velocity. At the rear of the model the energy exchange is smaller. The mass transfer occurs mainly by diffusion of dry ice molecules to the air stream. Therefore this part of the model shows a much smaller change in shape during the blow than the front part. At lower Mach numbers more dry ice evaporates due to the higher air densities.

24. There exist two possible explanations for the dependency of the evaporation rate on the model size. (a) The average thickness of the CO_2 air layer on the small model is smaller than on the large model, thus allowing a larger energy exchange relative to the size of the model. (b) Heat conducted from the model holder through the sting to the model has a greater influence on the overall evaporation from smaller models than from larger ones.

VII. CONCLUSIONS

25. The drag coefficient of dry ice spheres was found to be 1 at Mach numbers 4.25 and 2.87. It increased during the blow by 5 per cent at Mach number 4.25 and by 16 per cent at Mach number 2.87 due to the change of the sphere shape caused by evaporation. Within the accuracy of the drag measurements, the drag coefficient of dry ice models can be considered to be equal the drag coefficient of usual non-evaporative wind-tunnel models of the same shape. No influence of the evaporated CO_2 cloud on this coefficient was found.

26. The highest evaporation rate of CO_2 occurs on the front part of the models, showing a considerable change in the model shape in this region.

27. The specific mass loss due to the evaporation decreases with increasing model sizes and is the same for cubes and spheres within the measurement accuracy. Furthermore the specific mass loss increases with decreasing Mach numbers due to the increasing air densities in the test section of the tunnel.

VIII. REFERENCES

a. Thomas, R. N. and Whipple, F. L., "The Physical Theory of Meteors. II. Astroballistic Heat Transfer", The Astrophysical Journal, 114, 448, (1951)

b. Thomas, R. N. and Whipple, F. L., "Astroballistic Heat Transfer", Journal of Aeronautical Sciences, 18, 636 (1951)

c. Whipple, F. L., "Meteors and the Earth's Upper Atmosphere", Reviews of Modern Physics, 15, 246 (1943)

d. Communications with Professor Whipple

e. Kuiper, G. P., "The Atmospheres of the Earth and Planets", p. 149, Chicago 1949

f. Warfield, C. N., "Tentative Tables for the Properties of the Upper Atmosphere", NACA TN 1200 pp. 45, 51, Washington 1947

g. Lange, N. A., "Handbook of Chemistry", p. 1205, Sandusky, Ohio (1941)

h. Lightfoot, J. R., "The Naval Ordnance Laboratory Aeroballistic Research Facility", Naval Ordnance Laboratory Report (NOLR) No. 1079 (1950)

TABLE II

AVERAGE DECREASE OF THE MODEL DIAMETER[1] PERPENDICULAR TO THE AIR STREAM DURING TEST[2] AND DURING BLOW

Model	Mach Number	Diameter at Test Start	Diameter Loss During Test	Test Time[2]	Diameter at Blow Start	Diameter Loss During Blow	Blow Time
		mm	%	sec.	mm	%	sec.
sphere	4.25	48.3	4.4	475	46.9	1.1	35.3
	2.87	30.3	6.8	270	29.7	3.9	35.0
		50.6	5.1	325	49.7	2.9	37.7
		70.7	3.2	278	70.0	1.9	35.0
	1.86	31.2	12.8	297	30.5	9.8	35.0
		50.2	7.4	332	49.6	5.2	35.1
cube[3]	2.87	31.3	6.4	224	30.9	4.1	35.1
		49.8	4.5	399	48.6	1.8	35.2
		70.5	2.6	382	69.4	0.8	35.4
	1.86	31.0	10.5	280	30.3	5.3	35.1
		49.9	5.3	286	49.2	3.5	35.1
cylinder	2.87	31.0	4.0	230	30.5	1.6	35.1

1) All given values are average values
2) Time between first and second weighing of the model
3) Diameter means side length of cube

TABLE III DRAG COEFFICIENT AND MASS LOSS OF DRY ICE MODELS

Ma Undisturbed flow	Wind Tunnel Data	Model shape	Approx. model diameter[1]	Ave. deviat. of dia.[2]	Drag Coeff. C_D (blow start)	Ave. deviat. of C_D	Drag Coeff. C_D (blow end)	Ave. deviat. of C_D	Number of tests	Mass loss during blow[3]	Ave. deviat.[4]	No. of tests
			cm	%		%		%		g/s cm^2	%	
0	barom. press. (mm Hg) 765 temperature (°K) 297 Mass loss referred to surface area of spheres and cubes: (g/sec. cm^2) 0.000283 ± 6%	sphere	4 to 7	—						0.00113[5]		10
		cube	3 to 5	—						0.00170[5]		5
1.86	supply pressure (mm Hg) 748 temp. (°K) 284 in undisturbed flow: velocity (m/sec.) 483 pressure (mm Hg) 119 temperature (°K) 168 density (kg·s^2·m^{-4}) 00335	sphere	2.9	3	—	—	—	—	--	0.0494	21	4
		"	4.8	2	—					0.0496	14	4
		cube	2.9	3	—					0.0515	6	3
		"	4.8	1	—					0.0433	4	3
2.87	supply pressure (mm Hg) 764 temp. (°K) 283 in undisturbed flow: velocity (m/sec.) 594 pressure (mm Hg) 25.3 temperature (°K) 106 density (kg·s^2·m^{-4}) 0.0112	sphere	2.9	2	—					0.0257	11	3
		"	4.8	6	0.97	8	1.12	9	2	0.0199	12	5
		"	6.9	1	—					0.0147	8	3
		cube	3.0	1	—					0.0256	15	3
		"	4.8	2	—					0.0190	16	4
		"	6.9	1	—					0.0181	9	3
		cyl. (5 cm lg)	3.0	—	—					0.0393	—	1
4.25	supply pressure (mm Hg) 753 temp. (°K) 288 in undisturbed flow: velocity (m/sec.) 673 pressure (mm Hg) 3.6 temperature (°K) 62 density (kg·s^2·m^{-4}) 0.00272	sphere	4.7	6	1.00	2	1.14	3	9	0.00950	17	10

1) Ave. diameter during blow. Diameter in case of cube is substituted by average length of edge
2) Ave. deviation of diameter of the single tests vs. ave. diameter as given in column 4.
3) Mass loss is referred to 1 second blowing time and 1 cm^2 cross-sectional area of the model.
4) Deviation of mass loss of the single tests vs. Ave. loss as given in column 11.
5) Mass loss without blow.

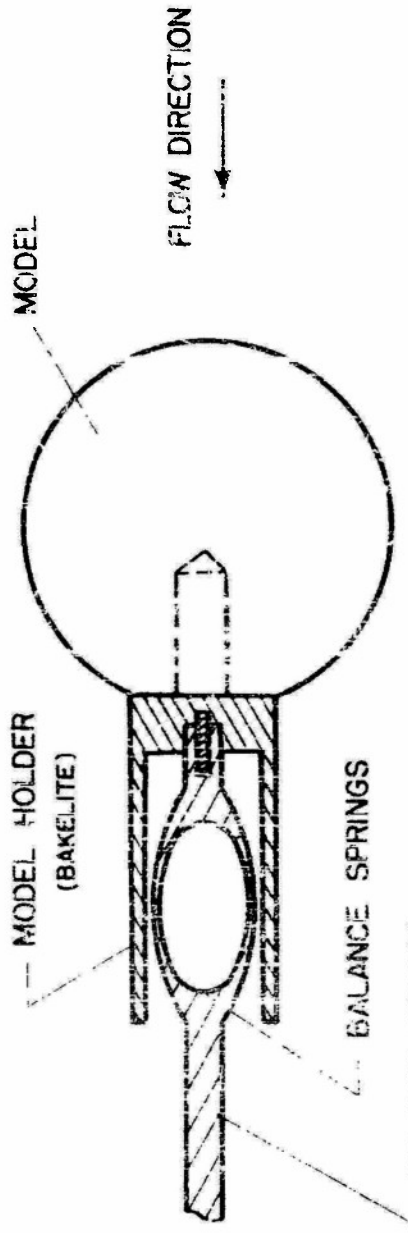

FIG. 1 MODEL MOUNTING

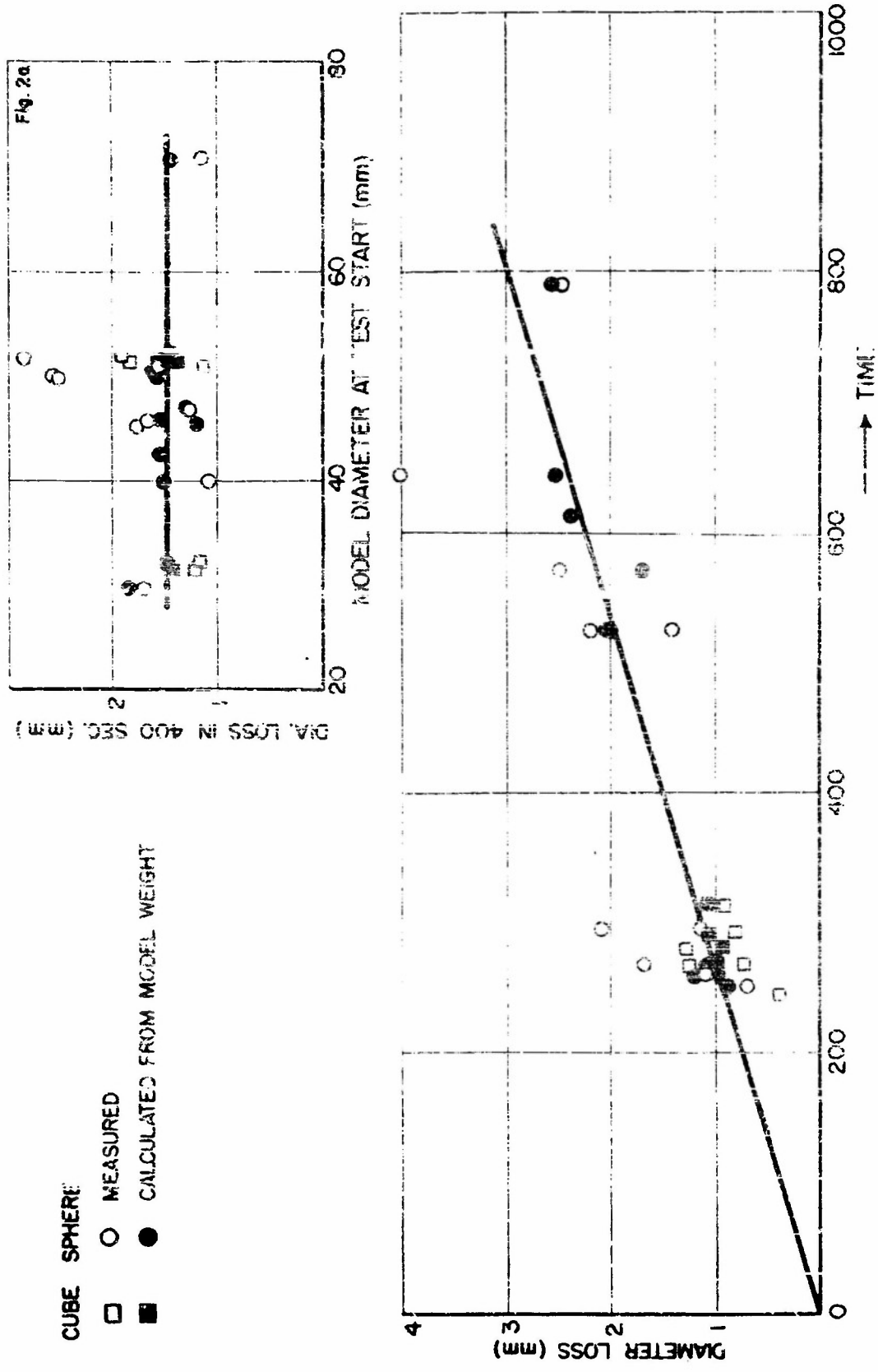

FIG. 2 DIAMETER DECREASE OF DRY ICE SPHERES AND CUBES WITHOUT BLOW

FLOW DIRECTION

MACH NUMBER 2.87

SPHERE CUBE

CYLINDER

MACH NUMBER 1.86

FIG. 3 MODEL SHAPES AT BLOW END

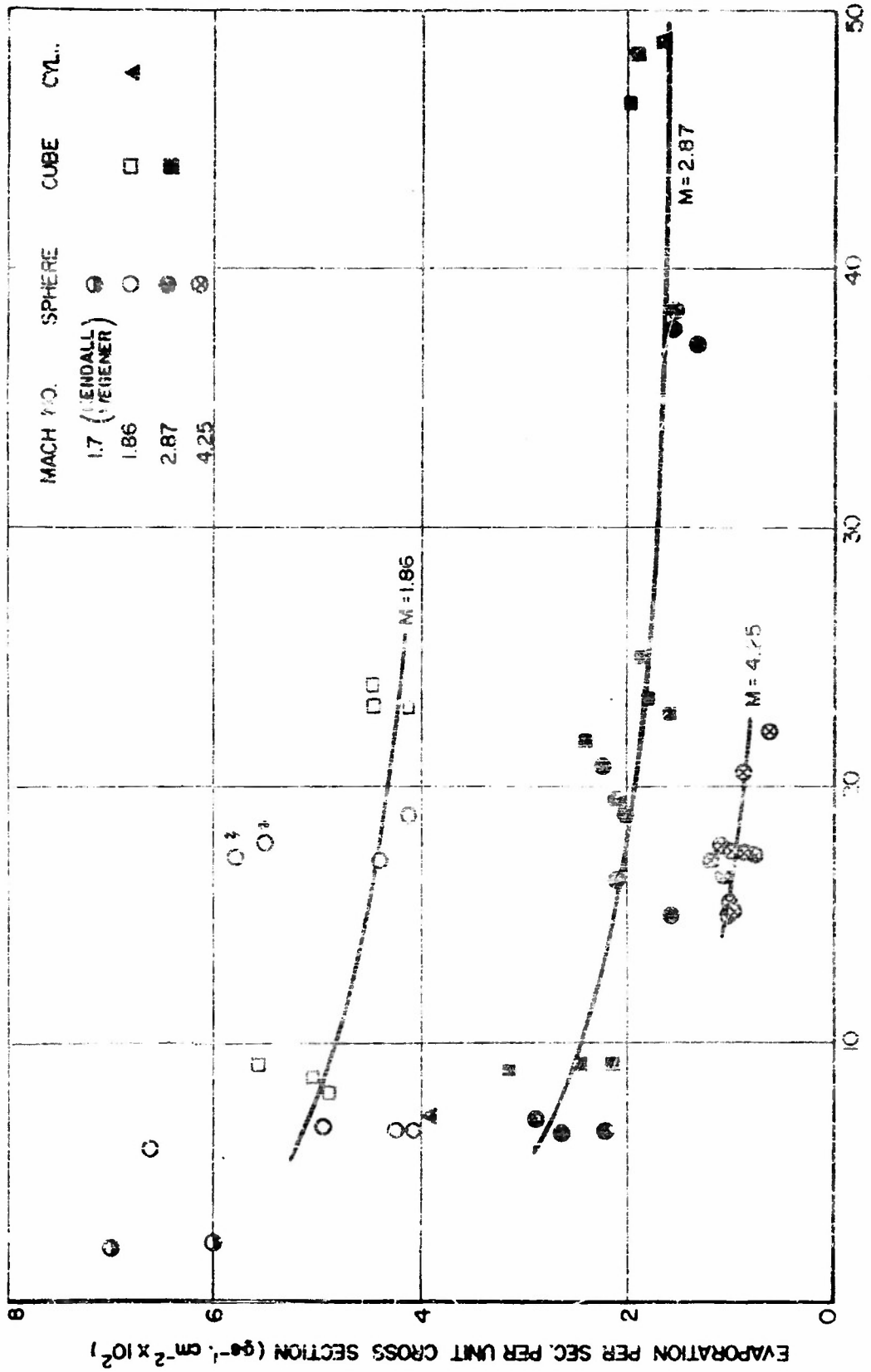

FIG 4 EVAPORATION OF CUBES AND SPHERES OF DRY ICE AT DIFFERENT MACH NUMBERS VS CROSS SECTIONAL AREA OF THESE BODIES

Aeroballistic Research Department
External Distribution List for Aeroballistics Research (XI)

No. of Copies	
	Chief, Bureau of Ordnance Department of the Navy Washington 25, D.C.
1	Attn: Rea
1	Attn: Rexc
1	Attn: Re3d
2	Attn: Re6
3	Attn: Re9a
	Chief, Bureau of Aeronautics Department of the Navy Washington 25, D. C.
1	Attn: AER-TD-414
2	Attn: RS-7
	Commander U. S. Naval Ordnance Test Station Inyokern P.O. China Lake, California
2	Attn: Technical Library
1	Attn: Code 5003
	Commander U.S. Naval Air Missile Test Center Point Mugu, California
2	Attn: Technical Library
	Superintendent U.S. Naval Postgraduate School Monterey, California
1	Attn: Librarian
	Commanding Officer and Director David Taylor Model Basin Washington 7, D. C.
2	Attn: Hydrodynamics Laboratory
	Chief of Naval Research Library of Congress Washington 25, D. C.
2	Attn: Technical Info. Div.
	Office of Naval Research Department of the Navy Washington 25, D. C.
1	Attn: Code 438
2	Attn: Code 463
	Director Naval Research Laboratory Washington 25, D. C.
1	Attn: Code 2021
1	Attn: Code 3800
1	Officer-in-Charge Naval Aircraft Torpedo Unit U.S. Naval Air Station Quonset Point, Rhode Island
	Office, Chief of Ordnance Washington 25, D. C.
1	Attn: ORDTU

No. of Copies	
2	Library Branch Research and Development Board Pentagon 3D1041 Washington 25, D.C.
	Chief, AFSWP P.O. Box 2610 Washington 25, D. C.
1	Attn: Technical Library
1	Chief, Physical Vulnerability Branch Air Targets Division Directorate of Intelligence Headquarters, USAF Washington 25, D. C.
	Commanding General Wright Air Development Center Wright-Patterson Air Force Base Dayton, Ohio
5	Attn: WCAPD
1	Attn: WCSD
2	Attn: WCSOR
2	Attn: WCRRN
1	Attn: WCACD
1	Attn: WCRRF
1	Director Air University Library Maxwell Air Force Base, Alabama
	Commanding General Aberdeen Proving Ground Aberdeen, Maryland
1	Attn: C.L. Poor
1	Attn: D.S. Dederick
	National Bureau of Standards Washington 25, D.C.
1	Attn: Nat'l Applied Math. Lab.
1	Attn: Librarian (Ord. Dev. Div.)
1	Attn: Chief, Mechanics Div.
	National Bureau of Standards Corona Laboratories (Ord. Dev. Div.) Corona, California
1	Attn: Dr. H. Thomas
	National Bureau of Standards Building 3U, UCLA Campus 405 Hilgard Avenue Los Angeles 24, California
1	Attn: Librarian
	University of California 711 Mechanics Building Berkeley 4, California
1	Attn: Dr. R. G. Folsom
1	Attn: Mr. G. J. Maslach
1	Attn: Dr. S. A. Schaaf
	VIA: InsMat

No. of Copies

California Institute of Technology
Pasadena 4, California
2 Attn: Librarian(Guggenheim Aero Lab)
1 Attn: Dr. H.T. Nagamatsu
1 Attn: Prof. M.S. Plesset
1 Attn: Prof. F. Goddard
1 Attn: Dr. Hans W. Liepman
VIA: BuAero Representative

College of Engineering
Cornell University
Ithaca, New York
1 Attn: Prof. A. Kantrowitz
VIA: ONR

University of Illinois
202 E. E. R. L.
Urbana, Illinois
1 Attn: Prof A. H. Taub
VIA: InsMat

1 Director
Inst. for Fluid Dynamics and Applied Math
University of Maryland
College Park, Maryland
VIA: InsMat

Massachusetts Inst. of Technology
Cambridge 39, Massachusetts
1 Attn: Prof. G. Stever
1 Attn: Prof. J. Kaye
VIA: InsMat

University of Michigan
Ann Arbor, Michigan
1 Attn: Prof. Otto Laporte
VIA: InsMat

University of Michigan
Willow Run Research Center
Ypsilanti, Michigan
1 Attn: L.R. Biasell
VIA: InsMat

University of Minnesota
Rosemount, Minnesota
1 Attn: J. Leonard Frame
1 Attn: Prof. N. Hall
VIA: Asst InsMat

The Ohio State University
Columbus, Ohio
2 Attn: G. L. Von Eschen
VIA: Ass't InsMat

Polytechnic Institute of Brooklyn
99 Livingston Street
Brooklyn 2, New York
1 Attn: Dr. Antonio Ferri
VIA: ONR

Princeton University
Princeton, New Jersey
1 Attn: Prof. S. Bogdonoff
1 Attn: Prof. L. Lees
VIA: ONR

No. of Copies

Massachusetts Inst. of Technology
Cambridge 39. Massachusetts
2 Attn: Project Meteor
1 Attn: Guided Missiles Library

1 Princeton University
Forrestal Research Center Library
Project Squid
Princeton, New Jersey

Armour Research Foundation
35 West 33rd Street
Chicago 16, Illinois
1 Attn: Engr. Mech. Div
VIA: ONR

Applied Physics Laboratory
The Johns Hopkins University
8621 Georgia Avenue
Silver Spring, Maryland
1 Attn: Arthur G. Norris
VIA: NIO

1 Cornell Aeronautical Lab., Inc.
4455 Genesee Street
Buffalo 21, New York
VIA: BuAero Rep.

1 Defense Research Laboratory
University of Texas
Box 1, University Station
Austin, Texas
VIA: InsMat

Eastman Kodak Company
50 W. Main Street
Rochester 4, New York
1 Attn: Dr. Herbert Trotter, Jr.
VIA: NIO

General Electric Company
Building #1, Campbell Avenue Plant
Schenectady, New York
1 Attn: Joseph C. Hoffman
VIA: InsMachinery

The Rand Corporation
1500 Fourth Street
Santa Monica, California
1 Attn: The Librarian
VIA: InsMat

Consolidated Vultee Aircraft Corp.
Daingerfield, Texas
1 Attn: J.E. Arnold
VIA: Dev. Contract Office

Douglas Aircraft Company, Inc.
3000 Ocean Park Boulevard
Santa Monica, California
1 Attn: Mr. E.F. Burton
VIA: BuAero Resident Rep.

No. of
Copies

North American Aviation, Inc.
12214 Lakewood Boulevard
Downey, California
2 Attn: Aerophysics Library
VIA: BuAero Representative

United Aircraft Corporation
East Hartford 8, Connecticut
1 Attn: Robert C. Sale
VIA: BuAero Representative

National Advisory Committee for Aero
1724 F Street, Northwest
Washington 25, D. C.
5 Attn: E. B. Jackson

Ames Aeronautical Laboratory
Moffett Field, California
1 Attn: H.J. Allen
2 Attn: Dr. A.C. Charters

NACA Lewis Flight Propulsion Lab.
Cleveland Hopkins Airport
Cleveland 11, Ohio
1 Attn: John C. Evvard

Langley Aeronautical Laboratory
Langley Field, Virginia
1 Attn: Theoretical Aerodynamics Div.
1 Attn: J. V. Becker
1 Attn: Dr. Adolf Buseman
1 Attn: Mr. C. H. McLellan
1 Attn: Mr. J. Stack

Harvard University
21 Vanserg Building
Cambridge 38, Massachusetts
1 Attn: Prof. Garrett Birkhoff

The Johns Hopkins University
Charles and 34th Streets
Baltimore 18, Maryland
1 Attn: Dr. Francis H. Clauser

New York University
45 Fourth Avenue
New York 3, New York
1 Attn: Professor R. Courant

1 Dr. Allen E. Puckett, Head
Missile Aerodynamics Department
Hughes Aircraft Company
Culver City, California

1 Dr. Gordon N. Patterson, Director
Institute of Aerophysics
University of Toronto
Toronto 5, Ontario, Canada
VIA: BuOrd (Ad8)

Aeroballistic Research Department
External Distribution List for Aeroballistics Research (XIa)

No. of Copies	
6	Office of Naval Research Branch Office Navy 100 Fleet Post Office New York, New York
	Commanding General Aberdeen Proving Ground Aberdeen, Maryland
1	Attn: Dr. B L. Hicks
	National Bureau of Standards Aerodynamics Section Washington 25, D C.
1	Attn: Dr. G.B Schubauer, Chief
	Ames Aeronautical Laboratory Moffett Field, California
1	Attn: Walter G. Vincenti
	University of California Observatory 21 Berkeley 4, California
1	Attn: Leland E. Cunningham VIA: InsMat
	Massachusetts Inst. of Technology Dept. of Mathematics, Room 2-270 77 Massachusetts Avenue Cambridge, Massachusetts
1	Attn: Prof. Eric Reissner VIA: InsMat
	Graduate School Aeronautical Engr. Cornell University Ithaca, New York
1	Attn: W.R. Sears, Director VIA: ONR
	Applied Math. and Statistics Lab. Stanford University Stanford, California
1	Attn: R.J. Langie, Associate Dir. VIA: Ass't InsMat
	University of Minnesota Dept. of Aeronautical Engr. Minneapolis, Minnesota
1	Attn: Professor R. Hermann VIA: Ass't InsMat
	Case Institute of Technology Dept. of Mechanical Engineering Cleveland, Ohio
1	Attn: Professor G. Kuerti VIA: ONR
	Harvard University 109 Pierce Hall Cambridge 38, Massachusetts
1	Attn: Professor R. von Mises

No. of Copies	
1	Prof. E. R. G. Eckert Department of Mechanical Engineering University of Minnesota Minneapolis 14, Minnesota
1	Prof. F. L. Whipple Harvard College Observatory 60 Garden Street Cambridge 38, Massachusetts
1	Dr. Richard N. Thomas Harvard College Observatory 60 Garden Street Cambridge 38, Massachusetts
1	Dr. G. R. Eber Holloman Air Development Center Alamogordo, New Mexico
1	Dr. P. P. Wegener Jet Propulsion Laboratory 4800 Oak Grove Drive Pasadena, California